AGU PUBLICATIONS

Paleoceanography

RESEARCH ARTICLE
10.1002/2014PA002769

Key Points:
- Clumped isotope proxy applied to Eocene/Oligocene foraminifera
- Majority of oxygen isotopes change at EOT due to ice volume, not cooling

Supporting Information:
- Text S1, Tables S1–S3, and Figures S1–S3
- Tables S4–S7

Correspondence to:
S. V. Petersen,
sierravp@umich.edu

Citation:
Petersen, S. V., and D. P. Schrag (2015), Antarctic ice growth before and after the Eocene-Oligocene transition: New estimates from clumped isotope paleothermometry, *Paleoceanography*, *30*, 1305–1317, doi:10.1002/2014PA002769.

Received 5 DEC 2014
Accepted 16 SEP 2015
Accepted article online 21 SEP 2015
Published online 26 OCT 2015

Antarctic ice growth before and after the Eocene-Oligocene transition: New estimates from clumped isotope paleothermometry

S. V. Petersen[1,2] and D. P. Schrag[1]

[1]Department of Earth and Planetary Sciences, Harvard University, Cambridge, Massachusetts, USA, [2]Now at Department of Earth and Environmental Sciences, University of Michigan, Ann Arbor, Michigan, USA

Abstract Across the Eocene-Oligocene transition, the oxygen isotopic composition ($\delta^{18}O$) of benthic and planktonic foraminifera increased by over 1‰. This shift is thought to represent a combination of global cooling and the growth of a large ice sheet on the Antarctic continent. To determine the contribution of each of these factors to the total change in $\delta^{18}O$, we measured the clumped isotopic composition of planktonic foraminifera tests from Ocean Drilling Program Site 689 in the Southern Ocean. Near-surface temperatures were ~12°C in the intervals 0–1.5 Myr before and 1–2 Myr after the major (Oi-1) transition, in agreement with estimates made using other proxies at nearby sites. Temperatures cooled by 0.4 ± 1.1°C between these intervals, indicating that the long-term change in $\delta^{18}O$ seen in planktonic foraminifera at this site is predominantly due to changes in ice volume. A larger instantaneous cooling may have occurred during Oi-1 but is not captured in this study due to sampling resolution. The corresponding change in the isotopic composition of seawater ($\delta^{18}O_{sw}$) is 0.75 ± 0.23‰, which is within the range of previous estimates, and represents global ice growth equivalent to roughly ~110–120% of the volume of the modern Antarctic ice sheet or ~80–90 m of eustatic sea level change.

1. Introduction

The Eocene-Oligocene transition (EOT) was first identified as a large increase in the oxygen isotopic composition ($\delta^{18}O$) of benthic foraminifera near the Eocene-Oligocene boundary. The isotopic shift was initially interpreted as a signal of global cooling [*Shackleton and Kennett,* 1975; *Kennett and Shackleton*, 1976]. However, if ice-free conditions were assumed, post-transition benthic $\delta^{18}O$ values required bottom water temperatures colder than modern, irreconcilable with the assumed greenhouse climate of the time [*Miller et al*., 1987]. Later evidence, such as the synchronous appearance of ice-rafted debris in the Southern Ocean [*Ehrmann and Mackensen*, 1992; *Zachos et al*., 1992; *Scher et al*., 2011], glacial diamictites on the Antarctic Peninsula [*Ivany et al*., 2005], and changes in the Antarctic weathering regime [*Robert and Kennett*, 1997] suggested that at least part of the $\delta^{18}O$ increase was due to ice sheet growth on Antarctica. Coastal sediments also document sea level fall across this transition [*Kominz and Pekar*, 2001; *Pekar et al*., 2002; *Katz et al*., 2008; *Miller et al*., 2009; *Cramer et al*., 2011; *Houben et al*., 2012], supporting the interpretation of continental ice growth at this time. Many studies have now attributed the isotopic shift to a combination of cooling and ice growth [*Zachos et al*., 1996; *Zachos et al*., 2001; *Coxall et al*., 2005; *Lear et al*., 2008; *Miller et al*., 2008; *Katz et al*., 2008; *Miller et al*., 2009; *Liu et al*., 2009; *Cramer et al*., 2009; *Peck et al*., 2010; *Pusz et al*., 2011; *Cramer et al*., 2011; *Wade et al*., 2012; *Bohaty et al*., 2012]. However, the relative contributions of temperature change and ice growth to the total $\delta^{18}O$ increase, which is observed globally and can be as great as 1.5‰ at some locations, have been difficult to quantify due to uncertainties in paleotemperature proxies.

Previous attempts at estimating the temperature change across the EOT using the Mg/Ca proxy were complicated by coincident changes in the carbonate saturation state of the oceans, which affects the uptake of Mg into biogenic calcite [*Elderfield et al*., 2006]. Initial measurements on benthic foraminifera suggested bottom water warming across the EOT, contrary to the cooling suggested by the $\delta^{18}O$ record [*Lear et al*., 2000; *Billups and Schrag*, 2003; *Lear et al*., 2004]. However, when changes in carbonate ion concentration were accounted for using Li/Ca ratios [*Lear and Rosenthal*, 2006; *Lear et al*., 2010; *Peck et al*., 2010; *Pusz et al*., 2011], or shallower sites were chosen to minimize the effects [*Lear et al*., 2008; *Katz et al*., 2008, 2011; *Wade et al*., 2012; *Bohaty et al*., 2012], Mg/Ca measurements instead suggested cooling across the EOT. This was

Table 1. Calculated Increase in $\delta^{18}O_{sw}$ Across the EOT, Compiled From Published Literature

Study	Location	Method	Increase in $\delta^{18}O_{sw}$
Lear et al. [2008]	Tanzania Drilling Sites (TDP11, 12, 17) (tropical)	Mg/Ca on pristine benthic and planktonic foraminifera	0.6‰
Katz et al. [2008]	Saint Stephens Quarry, Alabama (tropical)	Mg/Ca on benthic foraminifera	1.2‰
Liu et al. [2009]	High latitudes (SH: DSDP 511, 277, and ODP 1090; NH: DSDP 336 and 913)	TEX_{86} and $U^{k'}_{37}$ (surface)	0.4–0.85‰
Peck et al. [2010]	South Atlantic (ODP 1263)	Mg/Ca on *S. utilisindex*	0.6‰
Pusz et al. [2011]	South Atlantic (ODP 1090 and 1265)	Mg/Ca on benthic foraminifera, corrected for changes in $[CO_3^{2-}]$	0.75‰
Cramer et al. [2011]	New Jersey coast (SL record) and global compilation of core sites	Mg/Ca and $\delta^{18}O$ on benthic foraminifera and a backstripped sea level record	1.1–1.2‰
Bohaty et al. [2012]	Southern high latitudes (ODP 738, 744, and 748)	Mg/Ca on benthic foraminifera and *S. angiporoides*	0.45–0.75‰
This Study	Southern Ocean (ODP 689)	Clumped isotopes on *S. utilisindex* and *S. angiporoides*	0.75 ± 0.23‰

corroborated by organic temperature proxies not sensitive to changes in carbonate chemistry, which measured ~3–5°C of high-latitude surface water cooling [*Liu et al.*, 2009].

When these cooling estimates are removed from the $\delta^{18}O$ change at each site, the remaining change in $\delta^{18}O$ must be due to changes in the isotopic composition of seawater ($\delta^{18}O_{sw}$), which is an indicator of continental ice growth. Several studies combined $\delta^{18}O$ and Mg/Ca with stratigraphic records of sea level change to estimate changes in $\delta^{18}O_{sw}$ [*Katz et al.*, 2008; *Miller et al.*, 2009; *Cramer et al.*, 2011]. The change in $\delta^{18}O_{sw}$ has now been estimated at low and high latitudes using different proxies, and ranges from 0.4‰ to 1.2‰, with many observations falling between 0.6‰ and 0.75‰ (Table 1).

While many records document the shift in $\delta^{18}O$ at the EOT in either benthic or planktonic foraminifera, uncertainties in the isotopic composition of seawater, both in the late Eocene and through the EOT, preclude the direct translation of these records into either absolute temperature or ice volume estimates. In this study, we utilize the clumped isotope paleothermometer, a new proxy that relates temperature to the ordering of heavy carbon and oxygen isotopes within the carbonate lattice [*Eiler,* 2011, and references therein]. This paleothermometer can independently measure absolute temperature and $\delta^{18}O_{sw}$ and is not sensitive to changes in the carbonate ion concentration ($[CO_3^{2-}]$) [*Eagle et al.*, 2013], assuming the carbonate precipitated at equilibrium [*Hill et al.*, 2014]. Here this proxy is applied to planktonic foraminifera from Maud Rise (Ocean Drilling Program Site 689) in order to produce the first record of absolute temperature change in the Southern Ocean for this time period and directly quantify ice growth. Temperature and $\delta^{18}O_{sw}$ estimates from the clumped isotope paleothermometer will provide new, independent constraints on the long-studied question of Antarctic ice growth at the EOT.

2. Methods and Materials

2.1. Site Selection and Sampling

Ocean Drilling Program (ODP) Site 689 (64°N, 3°E, Maud Rise, Weddell Sea) was selected for this study due to its location proximal to Antarctica and for the previous work done at this site [*Kennett and Stott*, 1990; *Mackensen and Ehrmann*, 1992; *Mead and Hodell*, 1995; *Billups and Schrag,* 2002, 2003; *Bohaty et al.*, 2012]. ODP Hole 689B (modern depth = 2080 m, paleodepth = 1500 m at 35 Ma) [*Diester-Haass and Zahn*, 1996; *Bohaty et al.*, 2012] has continuous recovery across the EOT and has good carbonate preservation (>75% $CaCO_3$) [*Shipboard Scientific Party,* 1988; *Kennett and Stott*, 1990].

ODP Hole 689B was sampled from 110.22 to 129.37 mbsf (core sections 689B-12H-7 to 689B-14H-7), yielding 13 depth horizons with sufficient sample material spanning the EOT (Table S1 in the supporting information). Depth horizons may be grouped into four periods: Late Eocene (one sample), Pre-transition (five samples), Transition (two samples), and Post-transition (five samples). Although errors on individual temperatures measured with the clumped isotope paleothermometer are sometimes larger than the change in temperature we are trying to detect at the EOT, by combining samples into larger intervals, we can still effectively address smaller changes in temperature. No samples come immediately after the transition due to insufficient foraminiferal material. Calculated changes in temperature or $\delta^{18}O$ measured between the Pre-transition and

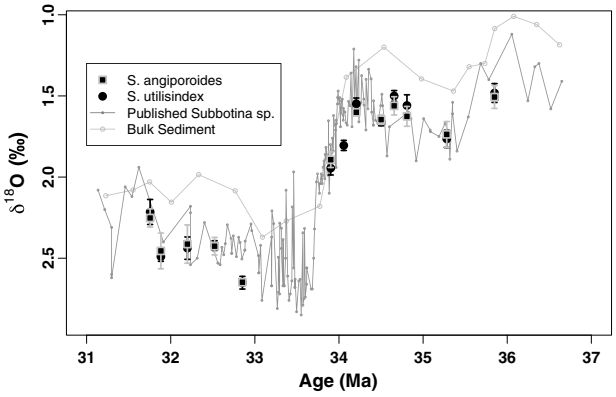

Figure 1. $\delta^{18}O$ of *S. angiporoides* and *S. utilisindex* versus age. Error bars denote 1 standard deviation of many replicates. Where only one replicate exists, the internal measurement error on that single point was used. Published $\delta^{18}O$ measured on *Subbotina sp.* is plotted for comparison. Data from 689D are plotted using authors' age model [*Bohaty et al.*, 2012], combined with data from 689B converted to the age model from this paper [*Stott et al.*, 1990; *Mackensen and Ehrmann*, 1992; *Robert and Kennett*, 1997]. Bulk sediment $\delta^{18}O$ is from *Shackleton and Hall* [1990].

Post-transition intervals should, therefore, be interpreted as a longer-term net change across the transition, as opposed to an instantaneous change at Oi-1.

2.2. Age Model

The age model for this core was created using chron positions from *SpeiB*, [1990] and *Florindo and Roberts* [2005], with age assignments from the most recent Geologic Time Scale [*Gradstein et al.*, 2012]. Depth and age information for the seven datums used for this age model can be found in Table S2. Sample ages were calculated by linear interpolation between the adjacent datums (Table S1). Using this age model, samples span 31.76 Ma to 35.85 Ma and the $\delta^{18}O$ transition (Oi-1) occurs at 33.70–34.15 Ma (see Figure 1).

2.3. Sample Preparation

Wet sediment was prepared for picking in the course of a previous study [*Billups and Schrag*, 2003], and the procedure is described by *Billups and Schrag* [2002]. For this study, the >63 μm fraction resulting from the prior sample preparation was dry sieved to capture the >150 μm size fraction only, from which foraminifera were individually picked. Due to the large sample material requirements of the clumped isotope procedure, we chose not to limit our sieved size range further. Although differences in stable isotopic composition between size fractions have been observed, the influence of test size on clumped isotopic composition has not yet been studied.

For each sample, two thermocline-dwelling planktonic species *Subbotina angiporoides* and *Subbotina utilisindex* were picked. In previous studies, these two species have been combined [*Mackensen and Ehrmann*, 1992; *Bohaty et al.*, 2012]. Here they are distinguished by *S. utilisindex* lacking the enveloping final chamber of *S. angiporoides* [*Jenkins and Orr*, 1973; *Pearson et al.*, 2006]. These species were chosen due to their abundance in Hole 689B around the EOT. Additionally, in one depth horizon, the surface-dwelling species *Chiloguembelina cubensis* was present in enough abundance to measure two replicates.

Picked foraminifera were sonicated for 20–30 s at a time and rinsed with deionized water to remove any caked sediment. This was repeated multiple times until the solute no longer became cloudy after sonication. Cleaned foraminifera were placed in an oven at 35°C to dry overnight. Dry foraminifera were separated into 1.1–2.5 mg aliquots for measurement, corresponding to ~150–300 tests per aliquot, with the majority of splits weighing 1.5–2.2 mg.

2.4. Clumped Isotope Measurement and Data Correction

The clumped isotope paleothermometer is based on the ordering of heavy oxygen and carbon isotopes within the carbonate lattice [*Eiler,* 2011, and references therein]. The level of "clumping" of these heavy isotopes is denoted by Δ_{47}, a value which compares the observed amount of mass-47 CO_2 (a CO_2 molecule containing both ^{13}C and ^{18}O) to that expected for a random (stochastic) distribution of atoms.

The clumped isotope measurement was made using a new high-efficiency sample preparation inlet and dual-reservoir measurement technique [*Petersen and Schrag*, 2014]. Foraminifera were reacted in phosphoric acid at 90°C, and then the resulting CO_2 was cleaned of contaminants by passing through a U-trap filled with Porapac Q material, held at −11°C. Finally, clean CO_2 was introduced into a Thermo Finnegan MAT 253 for analysis, equipped with five cups measuring masses 44 to 48 (with resistors of 3E7, 3E9, 1E10, 1E12, and 1E12 Ω, respectively). Samples were each run for 7–9 acquisitions of 14 cycles with 26 s integration time.

Raw voltages were converted to Δ_{47} using the calculations described by *Huntington et al.* [2009]. Measured Δ_{47} values of samples and carbonate standards were corrected to the absolute reference frame using heated gases (1000°C), and CO_2 equilibrated with water at 35°C and 10°C, as described by *Dennis et al.* [2011]. Carbonate standards whose values had been determined by previous studies [*Dennis et al.*, 2011; *Petersen and Schrag*, 2014] were run alongside samples. These included the in-house standards CM2 (Carrara marble, $\Delta_{47} = 0.395 \pm 0.005$‰) and RTG (tropical coral, $\Delta_{47} = 0.731 \pm 0.007$‰), and the international standard NBS19 (marble, $\Delta_{47} = 0.384 \pm 0.007$‰). Once in the absolute reference frame, carbonate data were corrected for fractionation during acid digestion using the 90°C acid digestion correction factor of 0.092‰ [*Henkes et al.*, 2013]. Reference frame-corrected Δ_{47} values of samples and standards were next corrected for a newly identified fractionation between Δ_{48} and Δ_{47} observed in the small-sample preparation procedure [*Petersen and Schrag*, 2014]. Finally, the $\Delta_{47\text{-corr}}$ values of unknowns were corrected for scale compression using a secondary transfer function made up of the carbonate standards, as described in *Meckler et al.* [2014].

Fully corrected Δ_{47} values were converted to temperature using the published calibration lines of *Ghosh et al.* [2006] (hereafter GH06) and *Dennis and Schrag* [2010] (hereafter DS10), both of which were updated to the absolute reference frame by *Dennis et al.* [2011]. These two calibrations cover the range of calibration equations that exist for this proxy [*Came et al.*, 2014, and references therein]. Two foraminifera-specific calibration studies exist [*Tripati et al.*, 2010; *Grauel et al.*, 2013] and show general agreement with the GH06 line, but at the time of comparison used data had not been corrected into the absolute reference frame. After correction into the absolute reference frame, foraminifera data from *Tripati et al.* [2010] fall between the updated GH06 and DS10 lines but are again much closer to GH06 [*Eagle et al.*, 2013]. We restrict our choice of calibrations to DS10 and GH06 because they represent the current range of uncertainty in calibrations.

2.5. Stable Isotope Measurements

Stable isotope measurements ($\delta^{18}O$ and $\delta^{13}C$) are acquired in the course of making the clumped isotope measurement. All isotope values for foraminifera are reported relative to Vienna Pee Dee Belemnite (VPDB). Oxygen isotope values were corrected for fractionation during the acid digestion step using the equation of *Swart et al.* [1991] for the common acid bath reaction method. Carbon isotope values and acid-corrected oxygen isotope values of unknowns were adjusted based on the mean offset of measured carbonate standards from known values for each measurement period. Average precision for $\delta^{13}C$ was 0.07‰ (1 standard deviation) for samples and standards. For $\delta^{18}O$, samples had a precision of 0.06‰ (1 standard deviation), whereas standards had a precision of 0.10‰ (1 standard deviation).

3. Results

3.1. $\delta^{18}O$ and $\delta^{13}C$

$\delta^{18}O$ and $\delta^{13}C$ values of *S. angiporoides* and *S. utilisindex* are statistically indistinguishable from each other (Table S4 and Figures 1 and S1). The high similarity between the two species supports the decision of previous authors to combine *S. angiporoides* and *S. utilisindex* [*Mackensen and Ehrmann,* 1992; *Bohaty et al.*, 2012]. In our study, each individual measured aliquot was made up of either *S. angiporoides* or *S. utilisindex*, but in later analysis, data from both species were combined within each depth horizon.

Measured $\delta^{18}O$ values for both species agree well with previously published data from this site (Figure 1). When taking into account the noise seen in high-resolution intervals, offsets of 0.1–0.2‰ in a few samples (689B-14H-7, 17 cm at 35.85 Ma and 689B-14H-2, 119 cm at 34.66 Ma) are likely attributable to the lower resolution of published $\delta^{18}O$ records in the intervals outside of the transition itself. Much of the high-resolution data covering the major shift in $\delta^{18}O$ was measured on Hole 689D and is plotted with the authors' age model [*Bohaty et al.*, 2012], which likely explains the horizontal offset seen in transition samples.

Across the EOT, $\delta^{18}O$ values increase by a maximum of 1.1‰, with an average increase of 0.82‰ between the Pre-transition and Post-transition periods (Table 2). The maximum change is similar to that observed in the previous high-resolution record from this site [*Bohaty et al.*, 2012], despite our lacking samples immediately after the transition. This is because our first Post-transition sample (689B-13H-4, 20 cm at 32.85 Ma) has a $\delta^{18}O$ value of 2.65‰, similar to the highest values previously measured immediately after the transition [*Stott et al.*, 1990; *Mackensen and Ehrmann,* 1992; *Robert and Kennett,* 1997; *Bohaty et al.*, 2012], but ~0.2‰ higher than published data of the same age. Post-transition $\delta^{18}O$ values decrease through time, capturing the "rebound" interval that is

Table 2. Mean Values for Four Time Intervals and the Change Between Pre-transition and Post-transition Intervals

Time Interval	Age Interval (Ma)	N	$\delta^{18}O$ (‰ VPDB)	Δ_{47} (‰)	Temperature (°C)[a]	$\delta^{18}O_{sw}$ (‰ VSMOW)[b]
Late Eocene	35.8	1	1.49 ± 0.02	0.708 ± 0.004	22.0 ± 1.5	3.26 ± 0.31
Pre-transition	35.3–34.2	5	1.62 ± 0.04	0.737 ± 0.003	12.3 ± 1.0	1.27 ± 0.22
Transition	33.9–34.1	2	1.87 ± 0.06	0.739 ± 0.005	11.6 ± 1.8	1.40 ± 0.44
Post-transition	31.8–32.9	5	2.44 ± 0.07	0.738 ± 0.002	11.9 ± 0.3	2.02 ± 0.06
Post-transition-Pre-transition change			0.82 ± 0.08	0.001 ± 0.003	−0.4 ± 1.1	0.75 ± 0.23

[a]Temperatures are calculated using the DS10 calibration [*Dennis and Schrag*, 2010; *Dennis et al*., 2011].
[b]$\delta^{18}O_{sw}$ values are calculated with DS10 temperatures and the equilibrium equation of *Kim and O'Neil* [1997].

also visible in the published data from this site [*Mackensen and Ehrmann,* 1992; *Robert and Kennett,* 1997; *Bohaty et al*., 2012] and in the global benthic stack [*Zachos et al*., 2001; *Cramer et al*., 2009].

$\delta^{13}C$ values gradually decrease from 1.5‰ to 1.1‰ toward the present, in general agreement with previously published studies [*Mackensen and Ehrmann*, 1992; *Mead and Hodell,* 1995; *Robert and Kennett*, 1997] (Figure S1). Transition samples are lower than published data, as is sample 689B-14H-3, 20 cm (34.81 Ma). However, only low-resolution $\delta^{13}C$ records exist for this site, which could explain these offsets. For both $\delta^{18}O$ and $\delta^{13}C$, stable isotope data from *S. angiporoides* and *S. utilisindex* differ substantially from bulk sediment stable isotope values (Figures 1 and S1) [*Shackleton and Hall*, 1990], suggesting our cleaning procedures were sufficient to remove any sediment attached to foraminifera tests.

In one sample (689B-14H-2, 67 cm, at 34.50 Ma), two replicates of *Chiloguembelina cubensis* were measured, giving $\delta^{13}C$ and $\delta^{18}O$ values of 1.998 ± 0.018‰ and 1.569 ± 0.040‰. This compares well with two measurements of this species at 122.06 and 122.8 mbsf that average to 2.10 ± 0.17‰ and 1.69 ± 0.07‰ [*Stott et al*., 1990]. At the same depth horizon, we measure $\delta^{13}C$ and $\delta^{18}O$ values of 1.429 ± 0.047‰ and 1.651 ± 0.028‰ for the combined *Subbotina* species.

3.2. Δ_{47} and Temperature

Δ_{47} values in our samples range from 0.708 to 0.745‰ (Figure 2), with all but the Late Eocene sample falling in an even narrower range of 0.728 to 0.745‰. Measurements of Δ_{47} from *S. utilisindex* and *S. angiporoides* were within error of each other in 10 out of 13 samples (Table S4 and Figure S3). In two samples (689B-13H-4, 20 cm at 35.28 Ma and 689B-14H-2, 119 cm at 34.66 Ma), mean Δ_{47} values for the two species did not overlap, and in a third sample (689B-14H-1, 68 cm at 34.06 Ma), there was not sufficient *S. angiporoides* to analyze. Δ_{47} values were converted to temperature for each individual replicate using the DS10 and GH06 clumped isotope calibrations, and average temperatures were calculated for each depth horizon by combining replicates of *S. utilisindex* and *S. angiporoides*. Temperatures calculated with the GH06 calibration were 8–10°C warmer than those calculated using the DS10 calibration (Figure S2). Excluding the Late Eocene sample, the average DS10 temperature was ~12°C, whereas the average GH06 temperature was ~22°C.

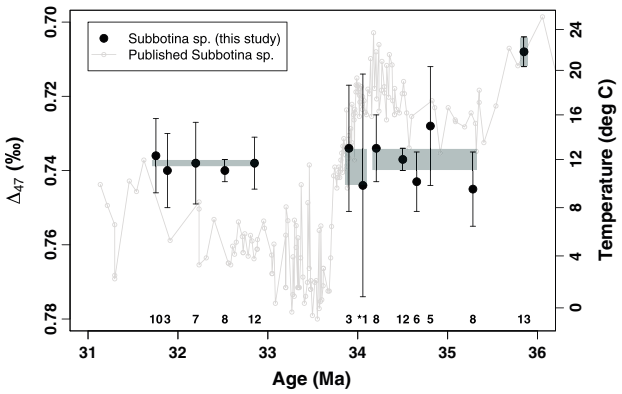

Figure 2. Δ_{47} versus age (black points) for *S. angiporoides* and *S. utilisindex* combined. Grey boxes indicate average values for four intervals described in the text. Error bars represent external 1 standard error of many replicates. * Where only one replicate is available, the fully propagated internal error on that measurement is used. The number of replicates per sample is shown along the bottom. A temperature axis (DS10 calibration) is shown on the right. High-resolution $\delta^{18}O$ from Figure 1 is plotted for reference (light grey) [*Stott et al*., 1990; *Mackensen and Ehrmann,* 1992; *Robert and Kennett*, 1997; *Bohaty et al*., 2012].

There is almost no change in Δ_{47} between the Pre-transition and Post-transition mean values (0.001 ± 0.003‰), indicating very little change in temperature across the EOT. Regardless of the calibration chosen, the net change

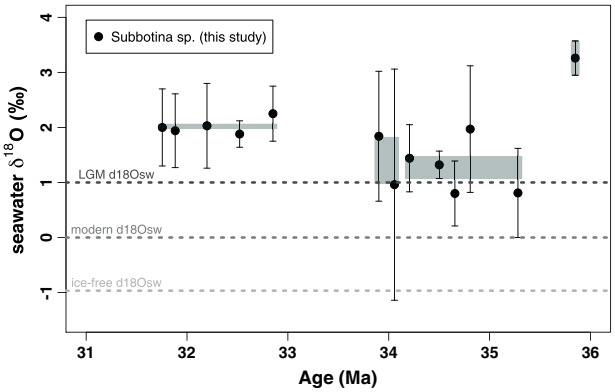

Figure 3. Calculated $\delta^{18}O_{sw}$ versus age $\delta^{18}O_{sw}$ values were calculated using the DS10 temperatures and the equilibrium equation of *Kim and O'Neil* [1997]. Approximate LGM, modern, and ice-free $\delta^{18}O_{sw}$ values are shown for comparison. Grey boxes indicate average values for four intervals described in the text.

in temperature between Pre-transition and Post-transition periods is the same, within error (GH06 = −0.4 ± 0.7°C, DS10 = −0.4 ± 1.1°C). In both cases, the data show a small cooling across the EOT.

The Late Eocene sample (689B-14H-7, 17 cm, at 35.85 Ma) has a Δ_{47} value of 0.708‰, outside the range of the other samples, suggesting warmer temperatures in the latest Eocene. This converts to a temperature of 22.0 ± 1.5°C using the DS10 calibration or 27.6 ± 0.9°C using GH06. In both calibrations, this sample indicates much warmer conditions at 35.8 Ma than in the Pre-transition and Post-transition intervals. This 5–10°C difference is not mirrored in $\delta^{18}O$ values, which are only 0.2‰ lower in the late Eocene than in the Pre-transition interval. The late Eocene value is made up of 13 analyses, made over two measurement periods. Despite being picked and cleaned at different times and corrected using different standard gases and carbonates, the mean values from the two measurement periods ($n = 6$ and $n = 7$) differ by 0.007 ± 0.009‰, within error of zero, suggesting that this is not a measurement artifact.

Comparison of the temperatures calculated using the two different calibrations with other proxies shows much better agreement with the DS10 temperatures (see section 4). This, combined with the fact that the DS10 calibration was performed in the same lab as this study using very similar procedures, lends credence to the DS10 temperatures over the GH06 temperatures in this case. For further calculations and discussion, we use the DS10 temperatures unless otherwise indicated.

In the one sample where *C. cubensis* was abundant enough for analysis (689B-14H-2, 67 cm), the two measured replicates recorded very disparate Δ_{47} values, resulting in a mean value with a very large error (0.699 ± 0.030‰). This is equivalent to a DS10 temperature of 25.7 ± 11.0°C. With an error so large, it is not possible to conclude anything about the environment of *C. cubensis* relative to the *Subbotina* species or to look at temperature gradients with depth.

3.3. $\delta^{18}O_{sw}$ and Ice Volume Estimates

Although $\delta^{18}O$ values change dramatically, both through the transition and within the rebound interval, Δ_{47} values remain nearly constant, requiring that the large change in foraminiferal $\delta^{18}O$ be accommodated completely by changes in the isotopic composition of seawater ($\delta^{18}O_{sw}$). $\delta^{18}O_{sw}$ was determined using the $\delta^{18}O$-temperature equilibrium relationship of *Kim and O'Neil* [1997] and the DS10 temperatures. All $\delta^{18}O_{sw}$ and $\delta^{18}O_{ice}$ values reported hereafter are relative to Vienna Standard Mean Ocean Water (SMOW). Calculated $\delta^{18}O_{sw}$ values range from 0.80‰ to 2.25‰, with the Late Eocene sample at 3.26‰ (Figure 3 and Table S4). The net change in $\delta^{18}O_{sw}$ between the Pre-transition and Post-transition intervals is 0.75 ± 0.23‰. This falls within the range of previous estimates made using other proxies at other sites (Table 1). Identical calculations done using the GH06-calculated temperatures yield higher absolute $\delta^{18}O_{sw}$ estimates (3.0‰ to 4.4‰) but the same net change (0.74 ± 0.14‰).

This change in $\delta^{18}O_{sw}$ can be converted to a change in sea level or a volume of continental ice by assuming an isotopic composition for the growing ice ($\delta^{18}O_{ice}$). Modeling studies estimate $\delta^{18}O_{ice}$ values ranging from −20 to −25‰ for initial late Eocene ice growth, to as low as −42‰ at the end of early Oligocene ice growth [*DeConto et al.*, 2008]. These estimates are significantly higher than the modern West and East Antarctic Ice Sheets, which have average compositions of −41 to −42.5‰ and −56.5‰, respectively [*Lhomme et al.*, 2005]. Using a range of $\delta^{18}O_{ice}$ values from −30‰ to −45‰, meant to represent the average ice sheet composition, a range of estimates of ice volume and sea level change was calculated (Table 3).

Table 3. Ice Growth Estimates Based On Different Isotopic Compositions of New Ice and the Measured Change in $\delta^{18}O_{sw}$ of 0.75 ± 0.23‰[a]

Average $\delta^{18}O_{ice}$	Mass of Ice ($\times 10^{19}$ kg)	Ice Volume ($\times 10^{7}$ km^3)	% Modern Antarctic Ice Sheet	Sea Level Change (m Eustatic Sea Level)
$\delta^{18}O_{ice} = -30$‰	3.5 ± 1.1	3.8 ± 1.2	143 ± 45%	106 ± 33
$\delta^{18}O_{ice} = -35$‰	3.0 ± 0.9	3.3 ± 1.0	122 ± 37%	91 ± 28
$\delta^{18}O_{ice} = -40$‰	2.6 ± 0.8	2.9 ± 0.9	107 ± 33%	79 ± 25
$\delta^{18}O_{ice} = -45$‰	2.3 ± 0.7	2.6 ± 0.8	95 ± 30%	71 ± 22

[a]Equations and values used in these calculations are detailed in the supporting information.

Using an intermediate value for $\delta^{18}O_{ice}$ (−35 to −40‰) and a change in $\delta^{18}O_{sw}$ of 0.75‰, we estimate 2.9–3.3 × 10^7 km^3 of ice growth, equivalent to 107–122% of the modern Antarctic ice sheet (AIS) volume (Table 3). This estimate is higher but consistent with modeling studies that have sustained ice sheets on the order of 2.1 × 10^7 km^3 on Antarctica under Eocene-Oligocene conditions [*DeConto et al.*, 2008]. At the EOT, the land area of Antarctica was 10–20% larger than today, which, based on the curvature of a growing ice sheet, would scale to an even greater increase in potential ice volume that could be housed on the continent [*Wilson and Luyendyk*, 2009]. In addition, any ice that was growing in the Northern Hemisphere or elsewhere at high elevation would reduce the volume that would need to be accommodated on the Antarctic continent.

The ice volume calculated from the intermediate $\delta^{18}O_{ice}$ composition may be converted into a eustatic sea level change by assuming a fixed ocean area (Table 3). Our estimate of 79–91 m eustatic sea level fall represents the long-term storage of ice on Antarctica 1–2 Myr after the EOT and is not directly comparable to other estimates of sea level change occurring at Oi-1. Nevertheless, our estimate is consistent with sedimentological evidence of 80 ± 25 m of eustatic sea level fall across the whole EOT [*Miller et al.*, 2009, and references therein].

4. Discussion

4.1. Comparison to Temperature Estimates From Other Proxies

Temperatures calculated in this study using the DS10 calibration are in line with temperature estimates made using other proxies at nearby sites. A multiproxy study including TEX_{86} and Δ_{47} measurements from Seymour Island (current location = 64°S, 56°W, paleolatitude = 67°S) reported temperatures at 34 Ma of 14.5 ± 1.4°C and 13.0 ± 1.5°C from the two proxies, respectively [*Douglas et al.*, 2014] (Figure 4). These agree well with our nearest data point (13.2 ± 2.8°C, 689B-14H-1, 118 cm, at 34.21 Ma) and Pre-transition average temperature (12.3 ± 1.0°C) (Table 2). Seymour Island is currently located at the same latitude as ODP Site 689 (64°S), and modeling studies suggest that these two sites would have experienced similar sea surface temperatures in the Eocene [*Douglas et al.*, 2014].

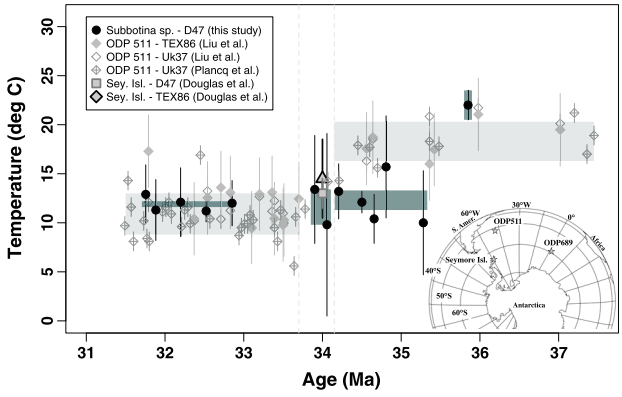

Figure 4. A comparison of Δ_{47}-derived temperatures (calculated using the DS10 calibrations) to TEX_{86} and $U^{k'}_{37}$ data from ODP511 [*Liu et al.*, 2009; *Plancq et al.*, 2014] and Δ_{47} and TEX_{86} data from Seymour Island [*Douglas et al.*, 2014]. Inset map shows modern locations of proxy sites. Vertical dashed lines mark the "transition" time interval, in which the majority of the $\delta^{18}O$ change occurs.

Temperature estimates also exist from site Deep Sea Drilling Project (DSDP) Site 511 (current location, 51°S, 46°W, paleolatitude = 52.5°S) in the South Atlantic, made using the TEX_{86} and $U^{k'}_{37}$ paleothermometers (Figure 4). DSDP Site 511 is subantarctic as opposed to ODP Site 689, which is truly polar. However, modeled Eocene surface circulation patterns include a clockwise gyre in the Weddell Sea that would have brought waters from along the Antarctic coast up the east coast of

South America [*Douglas et al*., 2014], potentially giving these two sites more similar temperatures than their latitudinal positions would suggest. The Pre-transition average temperature at DSDP Site 511 is 18.3 ± 2.0°C, covering the age range of 34.15–37.15 Ma [*Liu et al*., 2009; *Plancq et al*., 2014]. This is 6°C warmer than our Pre-transition average (12.3 ± 1.0°C, 34.2–35.3 Ma) but represents a period that extends further into the Eocene. In contrast, our Late Eocene sample (22.0 ± 1.5°C) is warmer than the DSDP Site 511 Pre-transition average but is within error of the two closest points (21.4 ± 1.9°C, 35.98 Ma) [*Liu et al*., 2009] and the average for an earlier interval (19.2 ± 0.5°C, 35.28–37.15 Ma) [*Liu et al*., 2009; *Plancq et al*., 2014]. The Post-transition average for DSDP Site 511 is 10.9 ± 2.1°C (31.5–33.7 Ma) [*Liu et al*., 2009; *Plancq et al*., 2014], in agreement with our Post-transition average (11.9 ± 0.3°C, 31.8–32.9 Ma).

Three proxies (Δ_{47}, TEX_{86}, and $U^{k'}_{37}$) now suggest subantarctic and Antarctic temperatures of 10–12°C in the early Oligocene [*Liu et al*., 2009; *Douglas et al*., 2014; *Plancq et al*., 2014] (this study). In high northern latitudes, similarly warm temperatures existed. In the Norwegian Sea (ODP Site 913, 75°N), TEX_{86}, methylation and cyclization of branched tetraethers (MBT index, CBT ratio), and pollen reconstructions record temperatures of 8–10°C, 10 ± 3°C, and 11 ± 2°C, respectively, for the early Oligocene [*Schouten et al*., 2008]. These temperatures may seem too warm, considering the many studies that now indicate a substantial Antarctic ice sheet at this time (Table 1). However, these high-latitude proxy reconstructions may be biased toward summertime temperatures due to light limitation during polar night [*Eldrett et al*., 2009]. For comparison, a modeling study found austral summertime (December-January-February) temperatures of ~4–7°C for 65°S with 2.5 × PAL CO_2 (700 ppm) and a full ice sheet on Antarctica, or ~7–11°C with no ice sheet [*Pollard and DeConto*, 2005].

4.2. Lack of Temperature Change at ODP Site 689

Most other studies of the Eocene-Oligocene transition record some amount of surface or deep cooling (2–5°C) across the transition, which is needed to account for the large magnitude change in $\delta^{18}O$ (>1.2‰) without requiring excessive ice growth. In contrast, the measurements on thermocline-dwelling *S. angiporoides* and *S. utilisindex* shown here record less than half a degree of cooling between Pre-transition and Post-transition intervals. Due to the spacing of samples around the EOT in this study, our calculated change in temperature represents a longer-term net change and does not capture any instantaneous changes across the transition. A larger cooling may have occurred during Oi-1 but would have to have mostly reversed by 32.85 Ma to be consistent with our first Post-transition sample. This reversal is seen in Mg/Ca data from the Kerguelan Plateau, which indicate a more pronounced cooling in the earliest Oligocene that reversed by 33 Ma, and in Mg/Ca data from ODP Site 689, which show a smaller syn-transition cooling that is reversed by 33.5 Ma (although this record ends before our first Post-transition sample, so direct comparison is impossible) [*Bohaty et al*., 2012]. Our estimate of long-term temperature change (−0.4 ± 1.1°C) allows for up to 1.5°C of cooling within error, which is compatible with other studies. This suggests that the long-term shift in $\delta^{18}O$ across the EOT was mainly the result of a semipermanent shift in continental ice volume, as opposed to significant cooling.

It is also possible that ocean waters did cool at this site, but that these thermocline-dwelling species did not record the cooling. The thermocline temperature could have remained the same, while the surface and/or deep water cooled, resulting in a shallower temperature gradient with depth. Alternatively, with or without a change in thermocline structure, *S. angiporoides* and *S. utilisindex* could have changed their depth habitat slightly to maintain the same thermal environment while ocean temperatures cooled. Such an adjustment would have been easier for these species than for surface-dwelling or benthic foraminifera due to the large thermal gradient found in the thermocline, requiring a much smaller change in depth (and therefore light conditions) to maintain the same temperature.

Regardless of whether the thermal gradient changed or these species adjusted their depth habitat to maintain the same thermal conditions, no change in temperature was recorded between the Pre-transition and Post-transition intervals. Therefore, assuming the ice volume signal was well mixed in the oceans, changes in $\delta^{18}O$ recorded in this study indicate global changes in $\delta^{18}O_{sw}$.

4.3. Extremely High $\delta^{18}O_{sw}$ Values

Despite the agreement between DS10-calculated temperatures and temperature estimates from other proxies at nearby sites, the $\delta^{18}O_{sw}$ values calculated using the DS10 temperatures are unreasonably high.

In the late Eocene, $\delta^{18}O_{sw}$ values are expected to be between −1 and 0‰, indicating the existence of only small, transient continental ice growth prior to the major ice growth event at the EOT [*Browning et al*., 1996; *Sagnotti et al*., 1998; *Tripati et al*., 2005]. This is nearly 2‰ lower than $\delta^{18}O_{sw}$ values calculated in this study. $\delta^{18}O_{sw}$ values of around +1‰ prior to the EOT ice growth require ice volumes in excess of the Last Glacial Maximum (LGM), when ice sheets covered large parts of North America. Unlike at the LGM, it is thought that in the Eocene, Northern Hemisphere ice was restricted to mountain glaciers only [*Edgar et al*., 2007; *Eldrett et al*., 2009], which is not sufficient to explain such high $\delta^{18}O_{sw}$ values. This discrepancy between calculated and expected $\delta^{18}O_{sw}$ values may be due to (1) errors in the absolute Δ_{47}-T calibration, producing temperatures that are too warm, (2) vital effects in these extinct species of foraminifera, resulting in $\delta^{18}O$ values enriched relative to equilibrium with seawater, or (3) diagenesis causing lower Δ_{47} and/or higher $\delta^{18}O$.

Differences in the Δ_{47}-T calibration would influence absolute temperature (and $\delta^{18}O_{sw}$) values but would have no impact on the calculated change in temperature, which would be near-zero regardless of the choice of calibration (as demonstrated by the equivalent change in temperature calculated by the GH06 and DS10 calibrations). The many published Δ_{47}-T calibrations tend to fall into two groups, those with steeper slopes similar to GH06 and those with shallower slopes similar to DS10 [*Came et al*., 2014, and references therein; *Tang et al*., 2014, and references therein]. Among the calibrations with the shallower DS10 slope, the intercept values differ by ~0.02–0.04‰ in the Δ_{47} range of interest [*Schauble et al*., 2006; *Dennis and Schrag*, 2010; *Henkes et al*., 2013; *Hill et al*., 2014; *Eagle et al*., 2013]. A decrease of 0.02‰ in the intercept of the calibration would result in a decrease of ~6°C for the mean temperature both before and after the transition (from ~12 to ~6°C in both periods). At these lower temperatures, $\delta^{18}O_{sw}$ values become −0.12‰ before the EOT and 0.63‰ after, showing the same magnitude of change (0.75‰), but absolute values much closer to those expected for a nearly ice-free Eocene. In order to get a Pre-transition $\delta^{18}O_{sw}$ value equal to the ice-free ocean end-member, the intercept would need to decrease by 0.031‰. However, at this point the calculated temperatures are 2–3°C, much lower than temperature estimates from other nearby proxies. Choice of the DS10 calibration over the other shallow slope calibrations with different intercepts is supported by the fact that the DS10 calibration was performed in the same lab as this study, eliminating the potentially biasing influence of any interlab differences in procedure.

Alternatively, the high $\delta^{18}O_{sw}$ values may be due to vital effects in *S. angiporoides* and *S. utilisindex* affecting $\delta^{18}O$. *Subbotina* species, including *S. angiporoides* and *S. utilisindex*, their ancestor *Subbotina linaperta* [*Pearson et al*., 2006], and others, often, but not always, record higher $\delta^{18}O$ (and lower $\delta^{13}C$) values than other planktonic foraminifera, resulting in their designation as thermocline dwellers [*Poore and Matthews*, 1984; *Keigwin and Corliss*, 1986; *Sexton et al*., 2006; *Wade and Pearson*, 2008]. For example, the size of the observed offset in $\delta^{18}O$ between *Subbotina* sp. and *Chiloguembelina cubensis* (the planktonic species often recording the lowest values) ranges from 0‰ up to 1.75‰ [*Poore and Matthews*, 1984; *Keigwin and Corliss*, 1986]. It is possible that instead of living in the cooler thermocline, *Subbotina* sp. were surface dwellers that incorporated more ^{18}O into their shells than would be expected from equilibrium with seawater (i.e., a vital effect), resulting in higher $\delta^{18}O$ and warm (surface) Δ_{47} temperatures. Such vital effects would have to increase $\delta^{18}O$ on the order of 1.5‰ above equilibrium to get reasonable $\delta^{18}O_{sw}$ values, given the temperatures measured in this study. Further work comparing clumped isotope temperatures of different species with the assumed habitats from $\delta^{18}O$ depth ranking could resolve these questions and strengthen paleoclimate interpretations. Typically, vital effects in foraminifera are expressed as a fixed offset from equilibrium values (e.g., +0.64‰ for *Cibicidoides* sp.) so would therefore only affect the absolute $\delta^{18}O$ and $\delta^{18}O_{sw}$ values but not the relative change in either across the EOT. There is no evidence for vital effects in Δ_{47} for foraminifera [*Tripati et al*., 2010].

Finally, the high $\delta^{18}O_{sw}$ values could be caused by diagenetic effects that increased either temperature or $\delta^{18}O$ values. Minimal resetting of $\delta^{18}O$ values is expected in high-latitude sites such as ODP 689 from modeling of sediment burial and pore water chemistry [*Schrag et al*., 1995]. Additional early precipitation of calcite in the colder environment of the seafloor or surface sediments would increase $\delta^{18}O$ but decrease Δ_{47} temperatures, resulting in little change in $\delta^{18}O_{sw}$. The samples in this study were taken from 110 to 130 mbsf and experienced temperatures of only ~6–13°C at these depths, according to limited downhole temperature data at ODP Sites 689 and 690 [*Nagao*, 1990]. Resetting of the clumped isotope signal by solid-state bond reordering only occurs at temperatures

above 100–150°C [*Henkes et al.*, 2014], much higher than those experienced by these samples. Recrystallization deep in the sediment column at temperatures of 6–13°C could possibly explain our Pre-transition and Post-transition data but cannot explain the late Eocene sample, which is 22°C.

4.4. Influence of Changing Carbonate Ion Concentrations on Ice Volume Estimates

Across the EOT, seawater carbonate ion concentration ($[CO_3^{2-}]$) has been calculated to change on the order of 36 μmol/kg in the deep Pacific [*Lear et al.*, 2010] to 19–29 μmol/kg in the South Atlantic [*Lear et al.*, 2010; *Peck et al.*, 2010] from paired Li/Ca and Mg/Ca measurements. These values agree with a change in $[CO_3^{2-}]$ of 19 μmol/kg calculated for a 1.2 km deepening of the carbonate compensation depth [*Lear et al.*, 2010; *Broecker and Peng*, 1982]. It has been shown that increases in $[CO_3^{2-}]$ cause reduced stable isotope values in planktonic foraminifera and other single-celled planktonic organisms with a slope of −0.0022‰ $\delta^{18}O$/(μmol/kg $[CO_3^{2-}]$) for *Orbulina universa* [*Spero et al.*, 1997], −0.0048 for a coccolithophore species, and −0.0243 for a calcareous dinoflagellate [*Ziveri et al.*, 2012]. Based on the above estimates of changes in $[CO_3^{2-}]$, this could influence $\delta^{18}O$ values by 0.04–0.08‰ for foraminifera, diminishing the full magnitude of the EOT signal. If instead the larger slope for coccolithophores was used, $\delta^{18}O$ values could be diminished by 0.09–0.17‰ across the transition. This influence would differ from site to site, basin to basin, and especially with depth of the core. A site like ODP Site 1218, which was near the CCD prior to the EOT [*Coxall et al.*, 2005], likely experienced a larger change in $[CO_3^{2-}]$ (36 μmol/kg) [*Lear et al.*, 2010], whereas a shallower site may have seen a smaller impact. These site-to-site and depth-dependent differences may explain some of the range in ice volume estimates shown in Table 1, because the calculated changes in $\delta^{18}O_{sw}$ may be variably muted according to the local change in $[CO_3^{2-}]$.

5. Conclusions

Clumped isotope measurements on Southern Ocean thermocline-dwelling foraminifera record a minor change in temperature (−0.4 ± 1.1°C) across the Eocene-Oligocene transition. Mean temperatures at site ODP Site 689 were 12.3°C before and 11.9°C after the transition, in line with temperature estimates from nearby sites [*Douglas et al.*, 2014; *Liu et al.*, 2009; *Plancq et al.*, 2014]. These temperatures represent average conditions in the 0–1.5 Myr before and 1–2 Myr after the main Oi-1 transition and may not capture the full change in temperature that occurred at the EOT. When combined with the change in $\delta^{18}O$, this cooling equates to a change in $\delta^{18}O_{sw}$ of 0.75 ± 0.23‰ between these intervals, equivalent to an ice volume increase of $2.9–3.3 \times 10^7$ km^3, or roughly 110–120% of the modern Antarctic ice sheet volume. These values are within the range of previous estimates (Table 2). The absolute values of $\delta^{18}O_{sw}$ are 1–2‰ higher than expected for this time period, which may be due to uncertainty in the Δ_{47}-T calibration and/or vital effects occurring in these species of foraminifera. Despite high absolute values, the calculated difference in $\delta^{18}O_{sw}$ is robust and is within the range of previous estimates. Overall, these results indicate that the longer-term shift in $\delta^{18}O$ across the EOT is due predominantly to a semipermanent shift in continental ice volume, and that any net temperature changes were less than ~1.5°C at this site. This result is not at odds with previous studies that measured greater cooling at the EOT. Larger instantaneous cooling could have occurred during the transition itself (not captured in this study) but must have mostly reversed by 32.75 Ma.

Acknowledgments
The data collected in this study are available in the supporting information. This work was supported by Henry and Wendy Breck and by the Harvard University GSAS Merit Fellowship. The authors would like to thank G. Eischeid, S. Manley, J. Shakun, and F. Chen for laboratory assistance. We would also like to thank two reviewers for their helpful comments.

References

Billups, K., and D. P. Schrag (2002), Paleotemperatures and ice volume of the past 27 Myr revisited with paired Mg/Ca and $^{18}O/^{16}O$ measurements on benthic foraminifera, *Paleoceanography*, *17*(1), 3-1–3-11, doi:10.1029/2000PA000567.

Billups, K., and D. P. Schrag (2003), Application of benthic foraminiferal Mg/Ca to questions of Cenozoic climate change, *Earth Planet. Sci. Lett.*, *209*(1–2), 181–195, doi:10.1016/S0012-821X(03)00067-0.

Bohaty, S. M., J. C. Zachos, and M. L. Delaney (2012), Foraminiferal Mg/Ca evidence for Southern Ocean cooling across the Eocene-Oligocene transition, *Earth Planet. Sci. Lett.*, *317–318*, 251–261, doi:10.1016/j.epsl.2011.11.037.

Broecker, W. S., and T.-H. Peng (1982), *Tracers in the Sea*, 169 pp., Lamont-Doherty Geological Observatory of Columbia Univ., Palisades, New York.

Browning, J. V., K. G. Miller, and D. K. Pak (1996), Global implications of lower to middle Eocene sequence boundaries on the New Jersey coastal plain: The icehouse cometh, *Geology*, *24*(7), 639–642, doi:10.1130/0091-7613(1996)024<0639:GIOLTM>2.3.CO;2.

Came, R. E., U. Brand, and H. P. Affek (2014), Clumped isotope signatures in modern brachiopod carbonate, *Chem. Geol.*, *377*, 20–30, doi:10.1016/j.chemgeo.2014.04.004.

Coxall, H. K., P. A. Wilson, H. Pälike, C. H. Lear, and J. Backman (2005), Rapid stepwise onset of Antarctic glaciation and deeper calcite compensation in the Pacific Ocean, *Nature*, *433*, 53–57, doi:10.1038/nature03135.

Cramer, B. S., J. R. Toggweiler, J. D. Wright, M. E. Katz, and K. G. Miller (2009), Ocean overturning since the Late Cretaceous: Inferences from a new benthic foraminiferal isotope compilation, *Paleoceanography*, *24*, PA4216, doi:10.1029/2008PA001683.

Cramer, B. S., K. G. Miller, P. J. Barrett, and J. D. Wright (2011), Late Cretaceous-Neogene trends in deep ocean temperature and continental ice volume: Reconciling records of benthic foraminiferal geochemistry (δ^{18}Oand Mg/Ca) with sea level history, *J. Geophys. Res.*, *116*, C12023, doi:10.1029/2011JC007255.

DeConto, R. M., D. Pollard, P. A. Wilson, H. Pälike, C. H. Lear, and M. Pagani (2008), Thresholds for Cenozoic bipolar glaciation, *Nature*, *455*, 652–657, doi:10.1038/nature07337.

Dennis, K. J., and D. P. Schrag (2010), Clumped isotope thermometry of carbonatites as an indicator of diagenetic alteration, *Geochim. Cosmochim. Acta*, *74*(14), 4110–4122, doi:10.1016/j.gca.2010.04.005.

Dennis, K. J., H. P. Affek, B. H. Passey, D. P. Schrag, and J. M. Eiler (2011), Defining an absolute reference frame for 'clumped' isotope studies of CO_2, *Geochim. Cosmochim. Acta*, *75*(22), 7117–7131, doi:10.1016/j.gca.2011.09.025.

Diester-Haass, L., and R. Zahn (1996), Eocene-Oligocene transition in the Southern Ocean: History of water circulation and biological productivity, *Geology*, *24*, 163–166, doi:10.1130/0091-7613(1996)024<0163:EOTITS>2.3.CO;2.

Douglas, P. M. J., H. P. Affek, L. C. Ivany, A. J. P. Houben, W. P. Sijp, A. Sluijs, S. Schouten, and M. Pagani (2014), Pronounced zonal heterogeneity in Eocene southern high-latitude sea surface temperatures, *Proc. Natl. Acad. Sci. U.S.A.*, *111*(18), 6582–6587, doi:10.1073/pnas.1321441111.

Eagle, R. A., et al. (2013), The influence of temperature and seawater carbonate saturation state on the ^{13}C-^{18}O bond ordering in bivalve mollusks, *Biogeosciences*, *10*(7), 4591–4606, doi:10.5194/bg-10-4591-2013.

Edgar, K. M., P. A. Wilson, P. F. Sexton, and Y. Suganuma (2007), No extreme bipolar glaciation during the main Eocene calcite compensation shift, *Nature*, *448*, 908–911, doi:10.1038/nature06053.

Ehrmann, W. U., and A. Mackensen (1992), Sedimentological evidence for the formation of an East Antarctic ice sheet in Eocene/Oligocene time, *Palaeogeogr. Palaeoclimatol. Palaeoecol.*, *93*(1–2), 85–112, doi:10.1016/0031-0182(92)90185-8.

Eiler, J. M. (2011), Climate reconstruction using carbonate clumped isotope thermometry, *Quat. Sci. Rev.*, *30*, 3575–3588, doi:10.1016/j.quascirev.2011.09.001.

Elderfield, H., J. Yu, P. Anand, T. Kiefer, and B. Nyland (2006), Calibrations for benthic foraminiferal Mg/Ca paleothermometry and the carbonate ion hypothesis, *Earth Planet. Sci. Lett.*, *250*(3–4), 633–649, doi:10.1016/j.epsl.2006.07.041.

Eldrett, J. S., D. R. Greenwood, I. C. Harding, and M. Huber (2009), Increased seasonality through the Eocene to Oligocene transition in northern high latitudes, *Nature*, *459*, 969–974, doi:10.1038/nature08069.

Florindo, F., and A. P. Roberts (2005), Eocene-Oligocene magnetobiochronology of ODP Sites 689 and 690, Maud Rise, Weddell Sea, Antarctica, *Geol. Soc. Am. Bull.*, *117*(1/2), 46–66, doi:10.1130/B25541.1.

Ghosh, P., J. Adkins, H. P. Affek, B. Balta, W. Guo, E. A. Schauble, D. P. Schrag, and J. M. Eiler (2006), ^{13}C-^{18}O bonds in carbonate minerals: A new kind of paleothermometer, *Geochim. Cosmochim. Acta*, *70*(6), 1439–1456, doi:10.1016/j.gca.2005.11.014.

Gradstein, F. M., J. G. Ogg, M. Schmitz, and G. Ogg (2012), Geomagnetic polarity time scale, in *The Geologic Time Scale 2012*, pp. 1176, Elsevier, Oxford, U. K., doi:10.1016/B978-0-444-59425-9.00005-6.

Grauel, A.-L., T. W. Schmid, B. Hu, C. Bergami, L. Capotondi, L. Zhou, and S. M. Bernasconi (2013), Calibration and application of the 'clumped isotope' thermometer to foraminifera for high-resolution climate reconstructions, *Geochim. Cosmochim. Acta*, *108*, 125–140, doi:10.1016/j.gca.2012.12.049.

Henkes, G. A., B. H. Passey, A. D. Wanamaker, E. L. Grossman, W. G. Ambrose, and M. L. Carroll (2013), Carbonate clumped isotope composition of modern marine mollusks and brachiopod shells, *Geochim. Cosmochim. Acta*, *106*, 307–325, doi:10.1016/j.gca.2012.12.020.

Henkes, G. A., B. H. Passey, E. L. Grossman, B. J. Shenton, A. Pérez-Huerta, and T. E. Yancey (2014), Temperature limits for preservation of primary calcite clumped isotope paleotemperatures, *Geochim. Cosmochim. Acta*, *139*, 362–382, doi:10.1016/j.gca.2014.04.040.

Hill, P. S., A. K. Tripati, and E. A. Schauble (2014), Theoretical constraints on the effects of pH, salinity, and temperature on clumped isotope signatures of dissolved inorganic carbon species precipitating carbonate minerals, *Geochim. Cosmochim. Acta*, *125*, 610–652, doi:10.1016/j.gca.2013.06.018.

Houben, A. J. P., C. A. van Mourik, A. Montanari, R. Coccioni, and H. Brinkhuis (2012), The Eocene-Oligocene transition: Changes in sea level, temperature, or both?, *Palaeogeogr. Palaeoclimatol. Palaeoecol.*, *335–336*, 75–83, doi:10.1016/j.palaeo.2011.04.008.

Huntington, K. W., et al. (2009), Methods and limitations of 'clumped' CO_2 isotope (Δ_{47}) analysis by gas-source isotope ratio mass spectrometry, *J. Mass Spectrom.*, *44*(9), 1318–1329, doi:10.1002/jms.1614.

Ivany, L. C., S. V. Simaeys, E. W. Domack, and S. D. Samson (2005), Evidence for an earliest Oligocene ice sheet on the Antarctic Peninsula, *Geology*, *34*(5), 377–380, doi:10.1130/G22383.1.

Jenkins, D. G., and W. N. Orr (1973), *Globigerina Utilisindex* n. sp. from the upper Eocene-Oligocene of the Eastern Equatorial Pacific, *J. Foram. Res.*, *3*(3), 133–136.

Katz, M. E., K. G. Miller, J. D. Wright, B. S. Wade, J. V. Browning, B. S. Cramer, and Y. Rosenthal (2008), Stepwise transition from the Eocene greenhouse to the Oligocene icehouse, *Nat. Geosci.*, *1*(5), 329–334, doi:10.1038/ngeo179.

Katz, M. E., B. S. Cramer, J. R. Togweiler, G. Esmay, C. Liu, K. G. Miller, Y. Rosenthal, B. S. Wade, and J. D. Wright (2011), Impact of Antarctic circumpolar current development on Late Paleogene ocean structure, *Science*, *332*(6033), 1076–1079, doi:10.1126/science.1202122.

Keigwin, L. D., and B. H. Corliss (1986), Stable isotopes in late middle Eocene to Oligocene foraminifera, *Geol. Soc. Am. Bull.*, *97*(3), 335–345, doi:10.1130/0016-7606(1986)97<335:SIILME>2.0.CO;2.

Kennett, J. P., and N. J. Shackleton (1976), Oxygen isotopic evidence for the development of the psychrosphere 38 Myr ago, *Nature*, *260*(5551), 513–515, doi:10.1038/260513a0.

Kennett, J. P., and L. D. Stott (1990), Proteus and Proto-Oceanus: Ancestral Paleogene oceans as revealed from Antarctic stable isotope results: ODP Leg 113, in *Proceedings of the Ocean Drilling Program, Scientific Results*, vol. 113, edited by P. Barker and J. P. Kennett, pp. 865–878, Ocean Drilling Program, College Station, Tex., doi:10.2973/odp.proc.sr.113.188.1990.

Kim, S.-T., and J. R. O'Neil (1997), Equilibrium and nonequilibrium oxygen isotope effects in synthetic carbonates, *Geochim. Cosmochim. Acta*, *61*(16), 3461–3475, doi:10.1016/S0016-7037(97)00169-5.

Kominz, M. A., and S. F. Pekar (2001), Oligocene eustasy from two-dimensional sequence stratigraphic backstripping, *Geol. Soc. Am. Bull.*, *113*(3), 291–304, doi:10.1130/0016-7606(2001)113<0291:OEFTDS>2.0.CO;2.

Lear, C. H., and Y. Rosenthal (2006), Benthic foraminiferal Li/Ca: Insights into Cenozoic seawater carbonate saturation state, *Geology*, *34*(11), 985–988, doi:10.1130/G22792A.1.

Lear, C. H., H. Elderfield, and P. A. Wilson (2000), Cenozoic deep-sea temperatures and global ice volumes from Mg/Ca in benthic foraminiferal calcite, *Science*, *287*(5451), 269–272, doi:10.1126/science.287.5451.269.

Lear, C. H., Y. Rosenthal, H. K. Coxall, and P. A. Wilson (2004), Late Eocene to early Miocene ice sheet dynamics and the global carbon cycle, *Paleoceanography*, *19*, PA4015, doi:10.1029/2004PA001039.

Lear, C. H., T. R. Bailey, P. N. Pearson, H. K. Coxall, and Y. Rosenthal (2008), Cooling and ice growth across the Eocene-Oligocene transition, *Geology*, *36*(3), 251–254, doi:10.1130/G24584A.1.

Lear, C. H., E. M. Mawbey, and Y. Rosenthal (2010), Cenozoic benthic foraminiferal Mg/Ca and Li/Ca records: Toward unlocking temperatures and saturation states, *Paleoceanography*, *25*, PA4215, doi:10.1029/2009PA001880.

Lhomme, N., G. K. C. Clarke, and C. Ritz (2005), Global budget of water isotopes inferred from polar ice sheets, *Geophys. Res. Lett.*, *32*, L20502, doi:10.1029/2005GL023774.

Liu, Z., M. Pagani, D. Zinniker, R. DeConto, M. Huber, H. Brinkhuis, S. R. Shah, R. M. Leckie, and A. Pearson (2009), Global cooling during the Eocene-Oligocene climate transition, *Science*, *323*(5918), 1187–1190, doi:10.1126/science.1166368.

Mackensen, A., and W. U. Ehrmann (1992), Middle Eocene through Early Oligocene climate history and paleoceanography in the Southern Ocean: Stable oxygen and carbon isotopes from ODP Sites on Maud Rise and Kerguelen Plateau, *Mar. Geol.*, *108*(1), 1–27, doi:10.1016/0025-3227(92)90210-9.

Mead, G. A., and D. A. Hodell (1995), Controls on the $^{87}Sr/^{86}Sr$ composition of seawater from the middle Eocene to Oligocene: Hole 689B, Maud Rise, Antarctica, *Paleoceanography*, *10*(2), 327–346, doi:10.1029/94PA03069.

Meckler, A. N., M. Ziegler, M. I. Millan, S. F. M. Breitenbach, and S. M. Bernasconi (2014), Long-term performance of the Kiel carbonate device with a new correction scheme for clumped isotope measurement, *Rapid Commun. Mass Spectrom.*, *28*(15), 1705–1715, doi:10.1002/rcm.6949.

Miller, K. G., R. G. Fairbanks, and G. S. Mountain (1987), Tertiary oxygen isotope synthesis, sea level history, and continental margin erosion, *Paleoceanography*, *2*(1), 1–19, doi:10.1039/PA002i001p00001.

Miller, K. G., J. V. Browning, M.-P. Aubry, B. S. Wade, M. E. Katz, A. A. Kulpecz, and J. D. Wright (2008), Eocene-Oligocene global climate and sea-level changes: St. Stephens Quarry, Alabama, *Geol. Soc. Am. Bull.*, *120*(1–2), 34–53, doi:10.1130/B26105.1.

Miller, K. G., J. D. Wright, M. E. Katz, B. S. Wade, J. V. Browning, B. S. Cramer, and Y. Rosenthal (2009), Climate threshold at the Eocene-Oligocene transition: Antarctic ice sheet influence on ocean circulation, *Geol. Soc. Am. Spec. Pap.*, *452*, 169–178, doi:10.1130/2009.2452(11).

Nagao, T. (1990), Heat flow measurements in the Weddell Sea, Antarctica: ODP Leg 113, in: *Proceedings of the Ocean Drilling Program, Scientific Results*, vol. 113, edited by P. Barker and J. P. Kennett, pp. 17–26, Ocean Drilling Program, College Station, Tex., doi:10.2973/odp.proc.sr.113.183.1990.

Pearson, P. N., R. K. Olsson, B. T. Huber, C. Hemleben, and W. A. Berggren (2006), Atlas of Eocene planktonic foraminifera, pp.514, Special Publication 41 (Cushman Foundation for Foraminiferal Research), Fredericksburg, Va.

Peck, V. L., J. Yu, S. Kender, and C. R. Riesselman (2010), Shifting ocean carbonate chemistry during the Eocene-Oligocene climate transition: Implications for deep-ocean Mg/Ca paleothermometry, *Paleoceanography*, *25*, PA4219, doi:10.1029/2009PA001906.

Pekar, S. F., N. Christie-Block, M. A. Kominz, and K. G. Miller (2002), Calibration between eustatic estimates from backstripping and oxygen isotopic records for the Oligocene, *Geology*, *30*, 903–906, doi:10.1130/0091-7613(2002)030<0903:CBEEFB>2.0.CO;2.

Petersen, S. V., and D. P. Schrag (2014), Clumped isotope measurements of small carbonate samples using a high-efficiency dual-reservoir technique, *Rapid Commun. Mass Spectrom.*, *28*, 2371–2381, doi:10.1002/rcm.7022.

Plancq, J., E. Mattioli, B. Pittet, L. Simon, and V. Grossi (2014), Productivity and sea-surface temperature changes recorded during the late Eocene-early Oligocene at DSDP Site 511 (South Atlantic), *Palaeogeogr. Palaeoclimatol. Palaeoecol.*, *407*, 34–44, doi:10.1016/j.palaeo.2014.04.016.

Pollard, D., and R. M. DeConto (2005), Hysteresis in Cenozoic Antarctic ice-sheet variations, *Global Planet. Change*, *45*, 9–21, doi:10.1016/j.gloplacha.2004.09.011.

Poore, R. Z., and R. K. Matthews (1984), Oxygen isotope ranking of Late Eocene and Oligocene planktonic foraminifers: Implications for Oligocene sea-surface temperatures and global ice-volume, *Mar. Micropaleontol.*, *9*, 111–134, doi:10.1016/0377-8398(84)90007-0.

Pusz, A. E., R. C. Thunell, and K. G. Miller (2011), Deep water temperature, carbonate ion, and ice volume changes across the Eocene-Oligocene climate transition, *Paleoceanography*, *26*, PA2205, doi:10.1029/2010PA001950.

Robert, C., and J. P. Kennett (1997), Antarctic continental weathering changes during the Eocene-Oligocene cryosphere expansion: Clay mineral and oxygen isotope evidence, *Geology*, *25*(7), 587–590, doi:10.1130/0091-7613(1997)025<0587:ACWCDE>2.3.CO;2.

Sagnotti, L., F. Florindo, K. L. Verosub, G. S. Wilson, and A. P. Roberts (1998), Environmental magnetic record of Antarctic palaeoclimate from Eocene/Oligocene glaciomarine sediments, Victoria Land Basin, *Geophys. J. Int.*, *134*, 653–662, doi:10.1046/j.1365-246x.1998.00559.x.

Schauble, E. A., P. Ghosh, and J. M. Eiler (2006), Preferential formation of ^{13}C-^{18}O bonds in carbonate minerals, estimated using first-principle lattice dynamics, *Geochim. Cosmochim. Acta*, *70*(10), 2510–2529, doi:10.1016/j.gca.2006.02.011.

Scher, H. D., S. M. Bohaty, J. C. Zachos, and M. L. Delaney (2011), Two-stepping into the icehouse: East Antarctic weathering during progressive ice-sheet expansion at the Eocene-Oligocene transition, *Geology*, *39*(4), 383–386, doi:10.1130/G31726.1.

Schouten, S., J. Eldrett, D. R. Greenwood, I. Harding, M. Baas, and J. S. Sinninghe Damste (2008), Onset of long-term cooling of Greenland near the Eocene-Oligocene boundary as revealed by branched tetraether lipids, *Geology*, *36*(2), 147–150, doi:10.1130/G24332A.1.

Schrag, D. P., D. J. DePaolo, and F. M. Richter (1995), Reconstructing past sea surface temperatures: Correcting for diagenesis of bulk marine carbonate, *Geochim. Cosmochim. Acta*, *59*(11), 2265–2278, doi:10.1016/0016-7037(95)00105-9.

Sexton, P. F., P. A. Wilson, and P. N. Pearson (2006), Palaeoecology of late middle Eocene planktic foraminifera and evolutionary implications, *Mar. Micropaleontol.*, *60*, 1–16, doi:10.1016/j.marmicro.2006.02.006.

Shackleton, N. J., and J. P. Kennett (1975), Paleotemperature history of the Cenozoic and the initiation of Antarctic glaciation: Oxygen and carbon isotope analyses in DSDP sites 277, 279, and 281, *Initial Rep. Deep Sea Drill. Project*, *29*, 743–755, doi:10.2973/dsdp.proc.29.117.1975.

Shackleton, N. J. and M. A. Hall (1990), Carbon isotope stratigraphy of bulk sediments, ODP sites 689 and 690, Maud Rise, Antarctica, in *Proceedings of the Ocean Drilling Program, Scientific Results*, vol. 113, edited by P. Barker and J. P. Kennett, pp. 985–989, Ocean Drilling Program, College Station, Tex., doi:10.2973/odp.proc.sr.113.211.1990,

Shipboard Scientific Party (1988), Site 689, in *Proc. of the Ocean Drill. Program Init. Rep,* vol. 113, edited by S. Baker et al., pp. 89–181, Ocean Drilling Program, College Station, Tex., doi:10.2973/odp.proc.ir.113.106.1988.

SpeiB, V. (1990), Cenozoic magnetostratigraphy of Leg 113 drill sites, Maud Rise, Weddell Sea, Antarctica, in *Proceedings of the Ocean Drilling Program, Scientific Results*, vol. 113, edited by P. Barker and J. P. Kennett, pp. 261–315, Ocean Drilling Program, College Station, Tex., doi:10.2973/odp.proc.sr.113.182.1990.

Spero, H. J., J. Bijma, D. W. Lea, and B. E. Bemis (1997), Effect of seawater carbonate concentration on foraminiferal carbon and oxygen isotopes, *Nature*, *390*(6659), 497–500, doi:10.1038/37333.

Stott, L. D., J. P. Kennett, N. J. Shackleton, and R. M. Corfield (1990), The evolution of Antarctic surface waters during the Paleogene: Inferences from the stable isotopic composition of planktonic foraminifers, ODP Leg 113, in *Proceedings of the Ocean Drilling Program, Scientific Results*, vol. 113, edited by P. Barker and J. P. Kennett, pp. 849–863, Ocean Drilling Program, College Station, Tex., doi:10.2973/odp.proc.sr.113.187.1990.

Swart, P. K., S. J. Burns, and J. J. Leder (1991), Fractionation of the stable isotopes of oxygen and carbon in carbon dioxide during the reaction of calcite with phosphoric acid as a function of temperature and technique, *Chem. Geol.*, *86*, 89–96, doi:10.1016/0168-9622(91)90055-2.

Tang, J., M. Dietzel, A. Fernandez, A. K. Tripati, and B. E. Rosenheim (2014), Evaluation of kinetic effects on clumped isotope fractionation (Δ_{47}) during inorganic calcite precipitation, *Geochim. Cosmochim. Acta*, *134*, 120–136, doi:10.1016/j.gca.2014.03.005.

Tripati, A. K., J. Backman, H. Elderfield, and P. Ferretti (2005), Eocene bipolar glaciation associated with global carbon cycle changes, *Nature*, *436*, 341–346, doi:10.1038/nature03874.

Tripati, A. K., R. A. Eagle, N. Thiagarajan, A. C. Gagnon, H. Bauch, P. R. Halloran, and J. M. Eiler (2010), ^{13}C-^{18}O isotope signatures and 'clumped isotope' thermometry in foraminifera and coccoliths, *Geochim. Cosmochim. Acta*, *74*(20), 5697–5717, doi:10.1016/j.gca.2010.07.006.

Wade, B. S., and P. N. Pearson (2008), Planktonic foraminiferal turnover, diversity fluctuations and geochemical signals across the Eocene/Oligocene boundary in Tanzania, *Mar. Micropaleontol.*, *68*, 244–255, doi:10.1016/j.marmicro.2008.04.002.

Wade, B. S., A. J. P. Houben, W. Quaijtaal, S. Schouten, Y. Rosenthal, K. G. Miller, M. E. Katz, J. D. Wright, and H. Brinkhuis (2012), Multiproxy record of abrupt sea-surface cooling across the Eocene-Oligocene transition in the Gulf of Mexico, *Geology*, *40*(2), 159–162, doi:10.1130/G32577.1.

Wilson, D. S., and B. P. Luyendyk (2009), West Antarctic paleotopography estimated at the Eocene-Oligocene climate transition, *Geophys. Res. Lett.*, *36*, L16302, doi:10.1029/2009GL039297.

Zachos, J., M. Pagani, L. Sloan, E. Thomas, and K. Billups (2001), Trends, rhythms, and aberrations in global climate 65 Ma to present, *Science*, *292*, 686–693, doi:10.1126/science.1059412.

Zachos, J. C., J. R. Breza, and S. W. Wise (1992), Early Oligocene ice-sheet expansion on Antarctica: Stable isotope and sedimentological evidence from Kerguelen Plateau, southern Indian Ocean, *Geology*, *20*, 569–573, doi:10.1130/0091-7613(1992)020<0569:EOISEO>2.3.CO;2.

Zachos, J. C., T. M. Quinn, and K. A. Salamy (1996), High-resolution (10^4 years) deep-sea foraminiferal stable isotope records of the Eocene-Oligocene climate transition, *Paleoceanography*, *11*(3), 251–266, doi:10.1029/96PA00571.

Ziveri, P., S. Thomas, I. Probert, M. Geisen, and G. Langer (2012), A universal carbonate ion effect on stable oxygen isotope ratios in unicellular planktonic calcifying organisms, *Biogeosciences*, *9*, 1025–1032, doi:10.5194/bg-9-1025-2012.